24 1x12 Wavelength-Selective Switches Using a 312-port 3D Waveguide and a Single 4k LCoS

Peter Wilkinson[1], Brian Robertson[1], Sam Giltrap[1], Oliver Snowdon[1], Harry Prudden[1], Haining Yang[1,2], Daping Chu[1,3]

1. Roadmap Systems Ltd, St John's Innovation Centre, Cowley Road, Cambridge, CB4 0WS, UK
2. Southeast University, 2 Sipailou, Xuanwu, Nanjing, Jiangsu, 210018, China
3. Department of Engineering, University of Cambridge, 9 JJ Thomson Avenue, Cambridge, CB3 0FA, UK
Author e-mail address: daping.chu@roadmapsystems.co.uk

Abstract: A switch module with a 4k LCoS is enabled by a 312-port waveguide array to produce 24 independent 1x12 WSSs. The average/best insertion losses were 8.4/7.2 dB, with crosstalk suppression of 26.9/40.5 dB.

OCIS codes: (060.6718) Switching, circuit; (090.2890) Holographic optical elements; (230.3720) Liquid-crystal devices; (230.7370) Waveguides.

1. Introduction

Wavelength-selective switches (WSSs) are core routing components of wavelength-division-multiplexed (WDM) reconfigurable optical networks [1,2]. Each WSS routes WDM channels between an input port and independently-selectable output ports, allowing centralised network control. WDM networks are increasingly using flexible spectrum allocation to maximise data capacity [3], causing pixelated liquid crystal on silicon (LCoS) devices to become the preferred WSS optical switching engine [4]. Our previous work has demonstrated that LCoS devices can effectively steer optical beams in 2D, using small square holograms [5]. This enables multiple independent WSSs to be integrated into a single module, sharing an LCoS device and bulk optical components [6]. This paper presents the next level of integration: a module with 24 independent 1x12 WSSs, using a single 4k LCoS device with a 6.8 µm pixel pitch. A 2D array of 312 input and output ports is required to implement a module of this size. A 3D laser-written glass waveguide is used to overcome the tolerance and yield issues of fabricating a 2D array of single-mode fibres (SMFs) on this scale. To our knowledge this is the first use of such a component to launch directed single-mode light into a free-space optical switch. The fabrication and optical performance of the waveguide array is detailed, together with the process for aligning it in the switch input assembly. The holographic optimisation and resultant performance of the assembled switch module are then described.

2. Optical Design

The optical architecture of the switch module is shown in Fig. 1(a). The architecture is split into two sections: the input assembly and the relay system. The input assembly is shown in Fig. 1(b). The waveguide contains a linear array of 24 port clusters on a 680 µm pitch. Each cluster corresponds to an individual WSS, and consists of 13 hexagonally-packed ports on an 80 µm pitch. The central port is the input, surrounded by the outputs. Each port has a corresponding collimating lenslet (L_S) of focal length 0.5474 mm proximal to the waveguide, and each cluster has a corresponding Fourier-transform (FT) lenslet (L_A) of focal length 3.427 mm distal to the waveguide. A beam waist of radius 68 µm is imaged at plane P_0 by lenslets L_A and L_S for each of the input ports, spread along the y-axis.

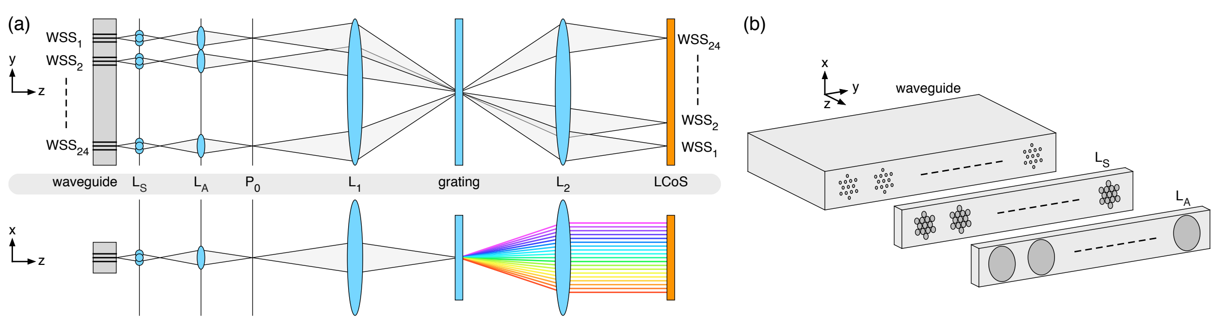

Fig. 1. (a) Optical architecture of the WSS module; (b) input assembly schematic.

The relay system uses two lenses (L_1 and L_2) of focal length 254.5 mm in a symmetric 4f configuration. These relay the waists from P_0 onto the reflective LCoS device. The beams from the 24 input ports are hence evenly spaced along the y-axis of the LCoS device. A diffraction grating with 1201.20 lines/mm at the central FT plane of the 4f relay disperses the wavelength channels along the x-axis of the LCoS device. An unmodulated beam covers 30x30 pixels on the LCoS device, and adjacent 50 GHz channels are separated by 50 pixels in the x-axis. The long axis of the 4k LCoS device is parallel with the x-axis, supporting 80 C-band channels of 50 GHz. Channel bandwidths can be adjusted in 1 GHz increments. The subholograms displayed on the pixels for each channel impart controllable angular deflections to the reflected beams, in both the xz and yz planes. The deflected return beams are then imaged at plane P_0 by the 4f relay. The wavelength channels from each input port are spatially coincident, having been re-multiplexed by the diffraction grating, but have different deflection angles. L_A converts these deflection angles into positional offsets at L_S. The deflection angle is controlled to steer the reflected beam into the target output port, where the corresponding L_S lenslet efficiently couples the beam into the waveguide. Polarisation-diversity optics are not included in the current module, but could easily be incorporated, as the LCoS fill factor is only 50% in the y-axis.

3. 3D Laser-Written Waveguide and Input Assembly

A 2D SMF array is not suitable for the 312-port array required for this WSS module, illustrated in Fig. 1(b). Fabrication tolerances on the SMF cladding diameter and core-cladding concentricity limit the achievable lateral and pointing errors of the input ports. For a previous 36-port array these errors averaged 1.87 µm and 0.27° [6], increasing switch insertion loss. Yield also decreases with port count, making larger arrays uneconomical. A laser-written glass waveguide from Optoscribe Ltd was therefore selected. Ultra-fast laser inscription used non-linear absorption to selectively alter the refractive index of small 3D elements in a dielectric substrate [7]. Multiple adjacent elements were combined to form waveguides with controllable 3D geometry. These waveguides map the 2D array of input ports in Fig. 1(b) on the front facet to a linear array on the rear facet, for butt-coupling to v-groove SMF arrays. This technique offers greater yield and better geometric tolerances for each port than a 2D SMF array. The average lateral error was measured as 0.61 µm, and the pointing error as 0.15°, as shown in Figs. 2(a) and (b). This type of waveguide had not previously been used for free-space applications, so the free-space beams were profiled. The mean ellipticity was 1.06, with the outliers in Fig. 2(c) corresponding to surface defects on the waveguide facet. The mean M^2 value for a sample of ports was 1.08, which to within the experimental error is indistinguishable from the 1.10 measured for an SMF. The free-space beam quality is hence equivalent to an SMF. The only drawback is insertion loss, as waveguides of this type have scattering and absorption losses of around 0.2 dB/cm. The average insertion loss for all channels from Fig. 2(d) was 1.69 dB. The average return loss was however only 3.04 dB, as the input ports had below-average insertion losses due to shorter path lengths. The central clusters had lower insertion losses for the same reason. This type of 3D waveguide therefore offers a viable replacement to SMFs for the input arrays of high-port-count WSSs.

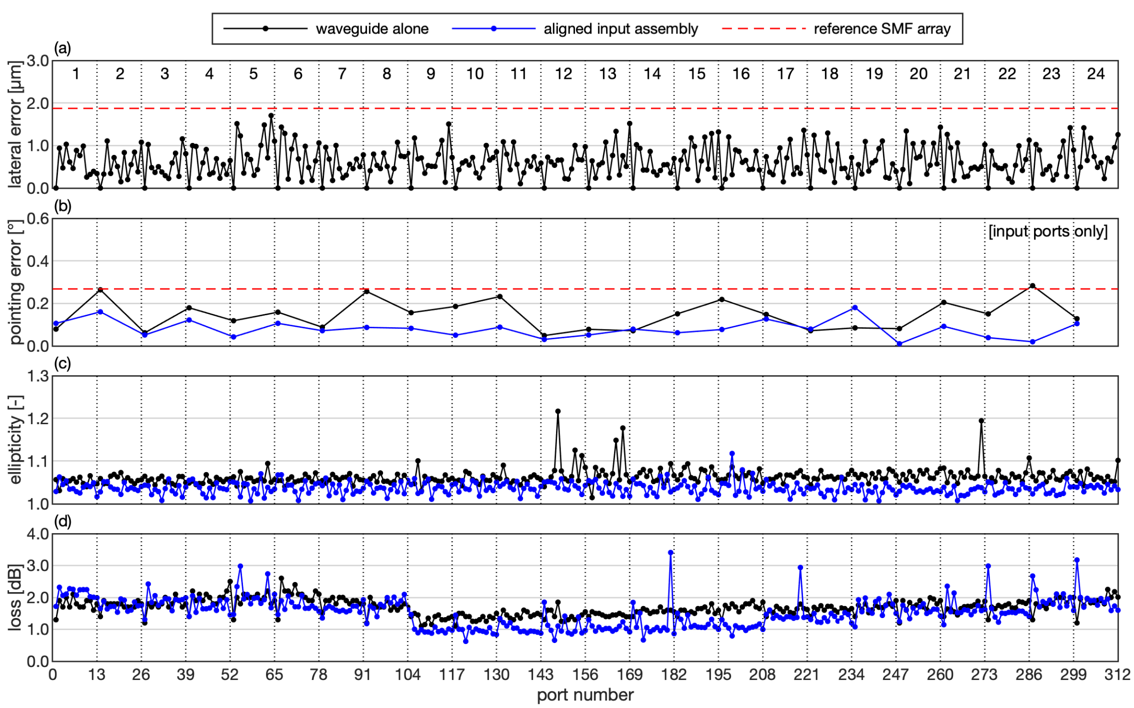

Fig. 2. (a) Lateral positioning errors of the waveguide core positions; (b) pointing errors of the input channel beams to the waveguide facet normal; (c) ellipticity of the free-space beams; (d) insertion losses from the input fibres to the free space beams.

The input array from Fig. 1(b) is long in the y-axis, with 15.64 mm between input ports 1 and 24. This makes the input assembly very sensitive to rotational misalignment of L_A and L_S about the z-axis, in addition to the usual lateral tolerances for efficient SMF coupling. A sequential active alignment procedure was therefore developed, together with the Tyndall National Institute. A mirror was set parallel to the waveguide front facet using a side-view camera. L_S was then inserted between the waveguide and the mirror, and parallelism set in the same way. The lateral alignment of each end of L_S was set by maximising back-reflection into the respective input ports from the mirror. L_S was then glued in place, and the procedure repeated for L_A. Figure 2 shows the performance of the completed input assembly. The expanded beam improved the pointing errors to an average of 0.09°. The average insertion loss fell to 1.52 dB, despite contamination increasing the loss for a few isolated ports. This apparent reduction was due to using a free-space power meter; the previous loss measurements were able to measure the power coupled into an SMF at the waveguide facet. The beam quality has also improved, with the average ellipticity dropping to 1.04, as the transparent adhesive between the waveguide and L_S reduced the impact of residual surface roughness on the waveguide facet. The sequential active alignment technique has hence satisfied the alignment tolerances required for such a large port array.

4. Holographic Optimisation and Switch Performance

The 2D output port configuration in Fig. 1(b) limits significant crosstalk to the -1 diffraction orders into the symmetrically-opposite ports. A high-dimensional optimisation of insertion loss and crosstalk was used to design the beam-steering subholograms. The resulting optical performance was consistent across the module, save for an increased insertion loss in WSSs 22-24 due to the contamination of the input ports. Example spectra for WSSs from a range of positions along the y-axis are shown in Fig. 3. The average insertion loss across all ports was 8.4 dB, with a range of 7.2 to 10.9 dB. The average crosstalk was -26.9 dB, varying from -19.6 to -40.5 dB. The average 3 dB passband on a 50 GHz channel was 43.4 GHz, ranging from 42.6 to 43.8 dB. Crosstalk between adjacent WSSs was less than -40 dB.

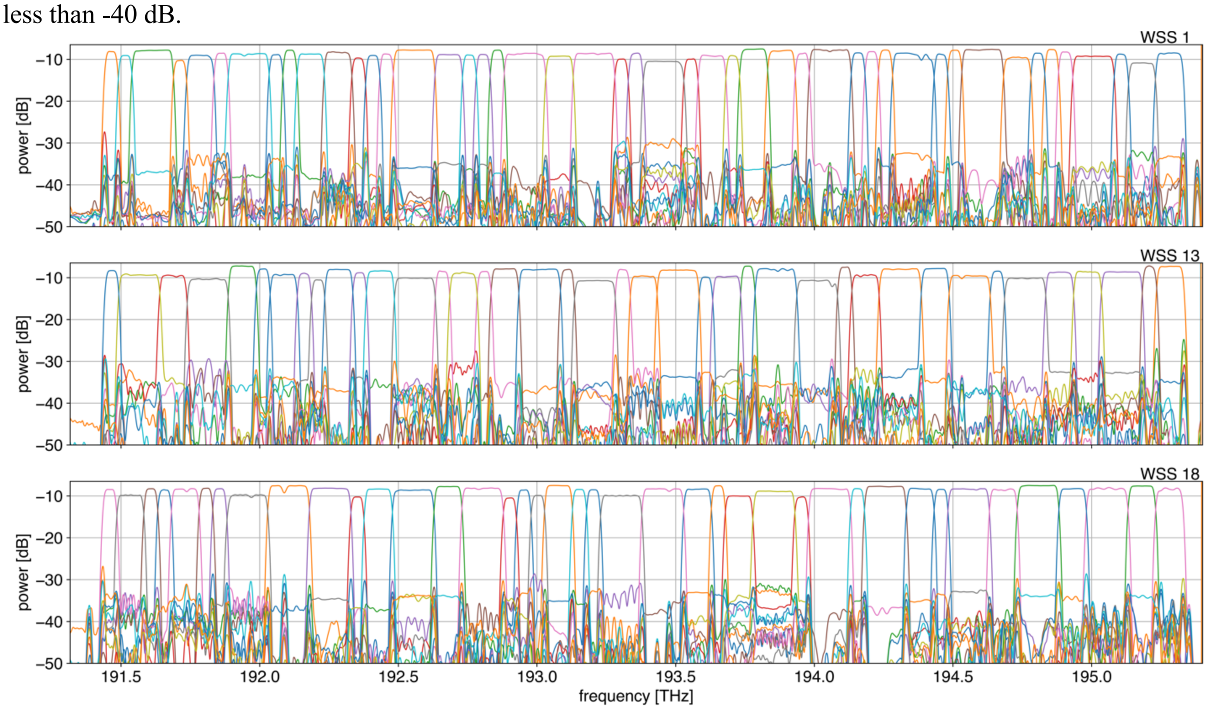

Fig. 3. Sample optical performance after high-dimensional optimisation.

The presented optical design, 3D waveguide port array, input assembly alignment technique and holographic optimisation have collectively enabled the realisation of a high-capacity WSS module using a 4k LCoS device. After accounting for the waveguide losses, the average optical system loss was 5.4 dB. There is scope to further reduce the waveguide loss, potentially by more than 1 dB. It is also believed that software and firmware improvements to the LCoS would allow the current maximum crosstalk suppression of circa 40 dB to be achieved across all channels.

5. References

[1] D. M. Marom, *et al.*, IEEE JLT **23**(4), 1620-1630 (2005).
[2] B. C. Collings, in OFC Tu3D.3 (2015).
[3] P. Wright, *et al.*, in ONDM (2013).
[4] S. Frisken, *et al.*, in OFC OTuM3 (2011).
[5] H. Yang, *et al.*, Optics Express **24**(11), 12240-12253 (2016).
[6] H. Yang, *et al.*, in OFC Th1J.2 (2018).
[7] D. Choudhury, *et al.*, Laser Photon Rev **8**(6), 827-846 (2014).